Arab J Geosci (2014) 7:2303–2314
DOI 10.1007/s12517-013-0858-9

ORIGINAL PAPER

Using artificial neural network (ANN) in prediction of collapse settlements of sandy gravels

H. Hasanzadehshooiili · Reza Mahinroosta · Ali Lakirouhani · Vahid Oshtaghi

Received: 18 August 2011 / Accepted: 25 January 2013 / Published online: 10 February 2013

Abstract Collapse settlement is one of the main geotechnical hazards, which should be controlled during first impoundment stage in embankment dams. Imposing large deformations and significant damages to dams makes it an important phenomenon, which should be checked during design phases. Also, existence of a variety of contributing parameters in this phenomenon makes it difficult and complicated to well predict the potential of collapse settlement. Thus, artificial neural networks, which are commonly applied by majority of geotechnical engineers in predicting various perplexing problems, can be efficiently used to calculate the value of collapse settlement. In this paper, feedforward backpropagation neural networks are considered. And three-layered FFBPNNs with the architectures of 4–6–2 and 4–9–2 accurately predicted the coefficient of stress release and collapse settlement value, respectively. These networks were trained using 180 datasets gained from large-scale direct shear test, which were carried out on gravel materials. High correlation between measured and predicted values for both collapse settlement and coefficient of stress release can be easily understood from the coefficient of determination and root mean square error. It is shown that sand content and normal stress applied to the specimens, respectively, are most effective parameters on the collapse settlement value and coefficient of stress release.

H. Hasanzadehshooiili (✉)
Department of Civil Engineering, Faculty of Engineering,
University of Guilan, Rasht, Guilan, Iran
e-mail: h.hasanzadeh.shooiili@gmail.com

R. Mahinroosta
Tarbiat Modares University, Tehran, Iran

A. Lakirouhani
Civil Engineering Department, University of Zanjan, Zanjan, Iran

V. Oshtaghi
Civil Engineering Department, University of Zanjan, Zanjan, Iran

Keywords Large-scale direct shear test · Artificial neural network · Collapse settlement of gravels · Coefficient of stress release

Introduction

When granular material becomes saturated, the in situ stresses, which have the role of confining pressure, suddenly decrease. And then, the particle's breakage may happen and cracks may develop in the grains. Breakage of particles bonds accompanies the stress reduction (Soroush and Aghaeiaraei 2005). As a consequence of this phenomenon, rearrangement of the broken particles will happen and collapse settlement will occur (Terzaghi 1960; Feda 1995; Alonso and Oldecop 2000; Hunter 2002; Soroush and Aghaeiaraei 2005). Nevertheless, the rate of strains will decrease after flooding (Marachi et al. 1969; Marsal 1973; Alonso and Oldecop 2000; Asadzadeh and Soroush 2009; Oshtaghi and Mahinroosta 2010).

The results of a significant number of laboratory tests indicated that collapse settlement degrades the strength parameters and deformation modulus of soils (Asadzadeh and Soroush 2009; Oshtaghi and Mahinroosta 2010; Alonso 2003; Soroush and Aghaeiaraei 2009; Kakoli and Hanna 2011; Haeri et al. 2012; Kim et al. 2012). This decrease is due to the weakening of particles leading to their breakage (Marsal 1967) and lubrication effects of water, which acts on the grain-to-grain contacts (Farmer and Attewell 1973; Touileb et al. 2000).

Collapse settlement is also important in central clay core of rockfill dams. Significant settlement in the upstream shells of such dams commonly occurs when the reservoir is filled. This can be 1–2 % of the height of dam (Naylor 1997). Also, it can be considerably more than the mentioned value in the cases that the quality of rockfill material is not

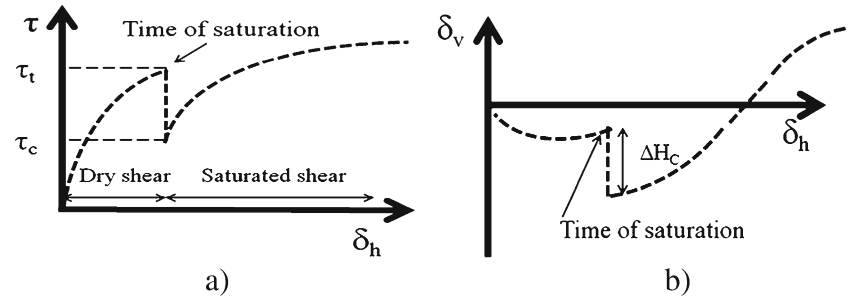

Fig. 1 **a** Shear stress versus horizontal displacement and **b** vertical displacement versus horizontal displacement of gravel specimens during collapse settlement test (Oshtaghi and Mahinroosta 2010)

so good (Baumann 1958; Naylor 1997). Collapse settlement may also be important in inundated road embankments or in reclaimed lands, where buildings are to be constructed. Nevertheless, the degree of importance of this phenomenon for rockfill dams is higher than embankments (Naylor 1997; Soriano and Sánchez 1999).

Figure 1 shows hypothetical stress and strain path for dry gravel in direct shear test. According to this figure, collapse factor, C, and the value of collapse settlement, ΔH_C, can be efficiently used in studying the collapse phenomenon (Oshtaghi and Mahinroosta 2010).

Collapse settlement factor can be used to model the stress reduction when the rockfill or the gravel material is saturated. Therefore, this factor which is also called coefficient of stress release, CSR, can be used to calculate the stress of the gravel in the saturated condition. By multiplying the stress of the material in the dry condition to the coefficient of stress release, the collapsed stress can be achieved. Thus, the collapse settlement factor can be obtained using Eq. (1) (Oshtaghi and Mahinroosta 2010):

$$\mathrm{CSR} = \frac{\tau_c}{\tau_t}. \tag{1}$$

In Eq. (1), τ_c is the collapse shear stress at the end of the impounding stage, when the collapse is completed, and τ_t shows dry shear stress of the specimen before the impounding stage.

CSR is related to the relaxation coefficient, "a", which was, firstly, introduced by Justo (1991) with the following equation:

$$\mathrm{CSR} = 1 - \mathrm{a} \tag{2}$$

where,

$$a = \frac{\tau_c + \tau_t}{\tau_t}. \tag{3}$$

There is a broad range of affecting parameters on the collapse settlement phenomenon such as initial water content, normal stress, shear stress level, sand soil content, clay content, relative density, number of impounding stages, etc. (Hunter 2002; Soroush and Aghaeiaraei 2005; Oshtaghi and Mahinroosta 2010). Contributing this wide range of parameters in this phenomenon makes it difficult to easily predict the value of the collapse settlement. Thus, in dire need of an inventive solution to predict this complicated function is completely obvious. High performance of artificial neural networks, a branch of artificial intelligence, and representing a precise solution for intricate situations have made it highly in demand in predicting several complicated problems. Artificial neural networks (ANNs) are broadly applied to a wide range of engineering and science complicated problems (Yang and Rosenbaum 2002; Neaupane and Adhikari 2006; Juang and Elton 1997; Yasrebi and Emami 2008; Monjezi et al. 2009; Hasanzadehshooiili et al. 2012a, b).

In this study, in order to predict the collapse settlement and the coefficient of stress release, an artificial neural network model is developed and the most affective parameters on these collapse parameters were gained by means of sensitivity analysis. Also, the effect of input parameters is investigated and results are compared by basic concepts in soil mechanics.

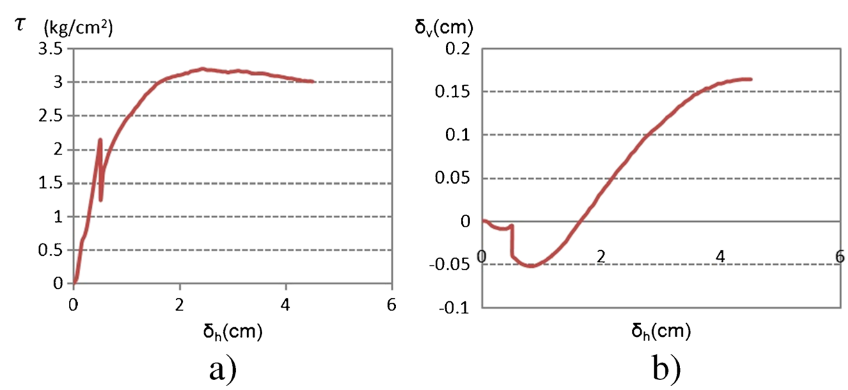

Fig. 2 **a** Shear stress and **b** vertical displacement versus horizontal displacement gained by large-scale direct shear test for vertical stress of 3 kg/cm^2, shear stress level of 50 %, and relative density of 85 % (Oshtaghi and Mahinroosta 2010)

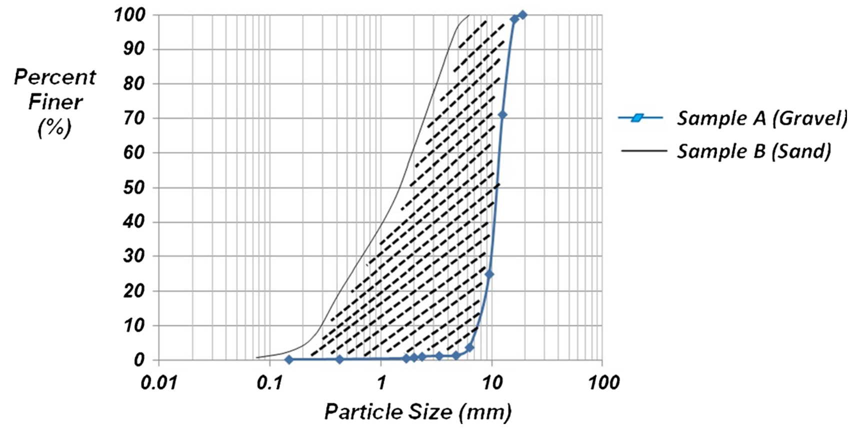

Fig. 3 Gradation range of studied material

Artificial neural network method

ANN is a branch of artificial intelligence, which its ability to calculate logic functions is firstly introduced by McCulloch and Pitts (1988). In this method, the accuracy of the model strongly depends on the database. The larger database results in the more accurate prediction (Maulenkamp and Grima 1999; Habibagahi and Taherian 2001; Khandelwal and Singh 2006; Monjezi et al. 2009). Indeed, an ANN model predicts values of desired outputs using some input parameters. To show the ability of ANN in the pattern recognition, Rosenblatt (1988) built a perceptron network. Multilayer perceptron (MLP), which is known as the best type of ANNs, is made up of three types of layers (input–hidden–output). It is documented that this type of neural networks can accurately approximate any type of the continuous function (Hornik 1989; Funahashi 1989). ANNs do not need any prior knowledge about the nature of relationships between the input/output variables, which is one of the benefits of ANNs in comparison to the most of the empirical and statistical methods (Yasrebi and Emami 2008). The number of layers depends on the complexity of the problem, which is to be solved. But, at least, one input, one output, and one hidden layer are required. Each layer contains some elements that are called neurons. These neurons are connected from one layer to the next one. But, there is not any connection between nodes of a specific layer. These nodes are connected using some links which have weight vectors. These weights are multiplied into processed information. And the sum of weighted input signals to each neuron is transformed by an activation function (Monjezi et al. 2010). To obtain the optimum model, the network has to be trained. After well training from a large number of datasets, network detects similarities and can predict the outputs while a new pattern is fed into the network (Khandelwal et al. 2004). A network has three major components that should be accurately assigned regarding the problem type, the transfer function, the learning law, and the network architecture (Simpson 1990).

Input and output parameters

In order to study the collapse settlement phenomenon and its affecting parameters, the large-scale direct shear test was considered. This test was carried out in the geotechnical laboratory of University of Zanjan using a 30×30×15-cm direct shear device. First of all, under a constant normal stress, dry gravel with a specific relative density was sheared to reach to a pre-assumed shear stress level. Then, in this level, the material was saturated. After well saturation, which was accompanied by the collapse settlement, the shearing process was continued to the failure of the gravel. For more clarifications about the actual behavior of the studied material, the shear stress and the vertical displacement variation versus the horizontal displacement are plotted in the normal stress of 3 kg/cm^2, shear stress level of 50 %, and relative density of 85 % in Fig. 2 (Oshtaghi and Mahinroosta 2010).

Table 1 Input and output parameters used in ANN

Type of data	Parameter	Symbol	Range
Inputs	Sand content (%)	SC	0–100
	Normal stress (kg/cm^2)	σ_n	1–5
	Shear stress level (%)	SL	30–100
	Relative density (%)	Dr	60–85
Outputs	Collapse settlement (mm)	ΔH	0.11–2.92
	Coefficient of stress release	CSR	0.289–0.779

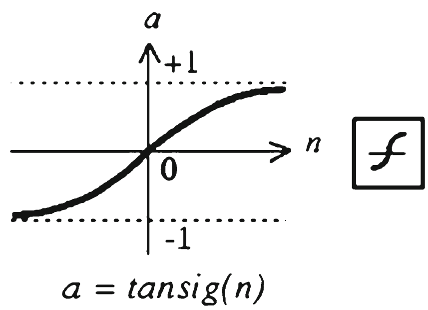

Fig. 4 Tan-sigmoid transfer function (Demuth et al. 1996)

As it was previously mentioned, there are lots of parameters affecting on the value of the collapse settlement. Thus, to comprehensively study the material's collapse behavior, the effect of all the concerning parameters should be considered. In this regard and relying on the literature, all the concerning parameters were sorted and were taken into account. And then, based on the material type, clean gravel (its gradation range is shown in Fig. 3), the influencing parameters were assigned. Among all the parameters with the most influence, due to the low variation in the samples' clay contents and stress paths, also, because of the constant value of the initial water content of the specimens, four parameters, which are commonly reported as the most influential parameters (Alonso and Oldecop 2000; Basma and Kallas 2004; Asadzadeh and Soroush 2009; Oshtaghi and Mahinroosta 2010), sand content, normal stress, shear stress level, and relative density, were considered as input parameters. Also, to investigate their effects on the value of the collapse settlement, using the large-scale direct shear test, the values of the collapse settlement and the coefficient of stress release were calculated as output parameters. It should be noted that in this study, the material's clay content does not significantly vary. Furthermore, the impounding stages and the initial water content of the samples remain constant.

On balance, input parameters, which their range of variation is shown in Table 1, are restricted to the sand content, normal stress, shear stress level, and relative density. In this study, a database including 180 datasets is prepared using the large-scale direct shear test. Also, the collapse settlement value and the coefficient of stress release are considered as output parameters, which are to be predicted by the network as desired values. The mentioned datasets are presented in Appendix 1.

Training the network

Backpropagation algorithm is widely suggested as the most efficient procedure in the training of neural networks. It has been implemented by a variety of researchers for learning procedure of their multilayer perceptron neural networks (Basma and Kallas 2004; Neaupane and Adhikari 2006; Yuan-Ping and Xiao-Yan 2007; Hasanzadehshooiili et al. 2012a, b). In this technique, in the forward pass, first of all, a specific value for connections between neurons is assigned. Afterward, in the backpropagation pass, the differences

Table 2 Results of comparison between some of the built models

No.	Architecture	RMSE	
		ΔH	CSR
1	(4–15–6–2)	0.206263	0.031432
2	(4–8–2)	0.154059	0.027494
3	(4–20–10–2)	0.148103	0.034656
4	(4–15–2)	0.138138	0.019409
5	(4–18–3–2)	0.136221	0.02171
6	(4–12–8–2)	0.130723	0.034064
7	(4–10–4–2)	0.127384	0.024837
8	(4–20–2)	0.120991	0.023225
9	(4–12–2)	0.115423	0.031315
10	(4–10–2)	0.107085	0.031738
11	(4–5–2)	0.094232	0.029996
12	(4–6–2)	0.092219	*0.01713*
13	(4–9–2)	*0.081711*	0.027887

Network with the architecture of 4-9-2 showing the minimum RMSE, presents the optimum network for predicting "ΔH". Also, the network architecture of 4-6-2 has the minimum RMSE in prediction of "CSR". Thus, the RMSE values of these two optimum networks were presented in italics

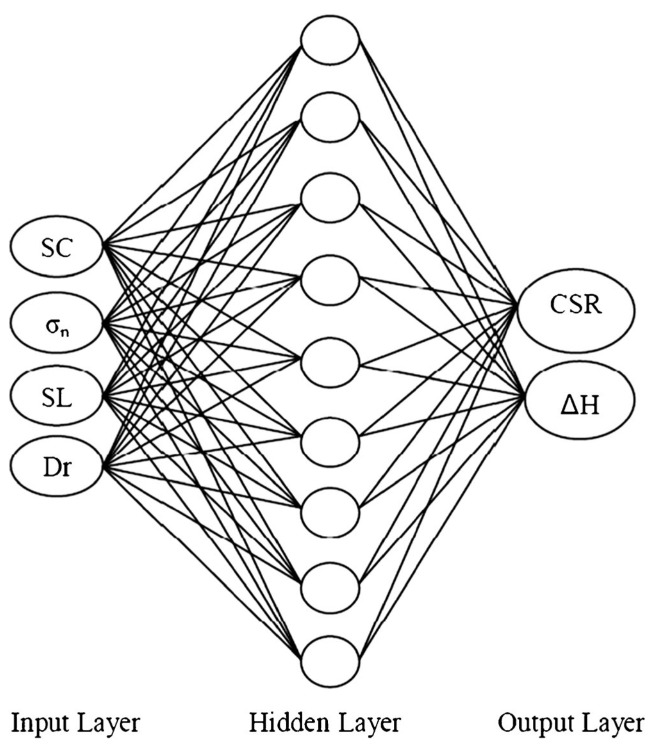

Fig. 5 Architecture of optimum model for predicting the value of ΔH

between predicted and measured values are calculated. Then, the error, which is calculated during forward pass, is back-propagated through the network to update the weights. The controlling parameter for this mechanism is a predefined threshold for the differences (Demuth et al. 1996; Yang and Rosenbaum 2002).

In order to build the model, at first, datasets were arranged and normalized in a scale of 0–1 using Eq. (4). Then, 90 % of datasets were considered as training datasets. The remaining was kept as the test datasets.

$$\text{Scaled value} = (\text{unscaled value} - \text{min value}) / (\text{max value} - \text{min value}). \quad (4)$$

After a large number of trials on different networks, the nonlinear tangent sigmoid function, TANSIG, showing the minimum error was considered as the transfer function for all the layers. Figure 4 shows the nonlinear TANSIG transfer function. Also, its formula is presented in Eq. (5) (Demuth et al. 1996).

$$f = \frac{e^{e_x} - e^{-e_x}}{e^{e_x} + e^{-e_x}} \quad (5)$$

where e_x is the weighted sum of the inputs for a processing unit.

As an important point, during the training process, two main phenomena should be considered: overfitting and underfitting. Overfitting, which makes the network memorize the outputs, occurs when a significant number of epochs are used during the training process. Also, if there is insufficient number of epochs used to train the network, the results will be underfitted and will lead to the model's inaccuracy (Maulenkamp and Grima 1999).

Network architecture

The best architectures of neural networks are gained by means of modeling a variety of one and two hidden layer neural networks and comparing their values of root mean square error (RMSE) and mean absolute error (MAE) (Hornik 1991; Pearson et al. 1995; Monjezi and Dehghani 2008).

RMSE and MAE are calculated using Eq. (6) and Eq. (7), respectively:

$$\text{RMSE} = \sqrt{\frac{\sum (\text{O}_\text{i} - \text{T}_\text{i})^2}{\text{N}}} \quad (6)$$

$$\text{MAE} = \left| \sum (\text{T}_\text{i} - \text{O}_\text{i}) \right| \quad (7)$$

where O_i and T_i represents the predicted and the measured outputs, respectively. Also, N is the number of data pairs. As shown in Table 2 for CSR, a network with the architecture of 4–6–2 having the minimum value of RMSE is the optimum one. Also, it can be seen that the topology 4–9–2 has the minimum RMSE for ΔH and therefore is the optimum model.

For the optimum models gained for CSR and ΔH, MAE was equal to 0.013 and 0.062 mm, respectively. Also, for better understanding of the network, schematic architecture of the optimum network for ΔH is shown in Fig. 5.

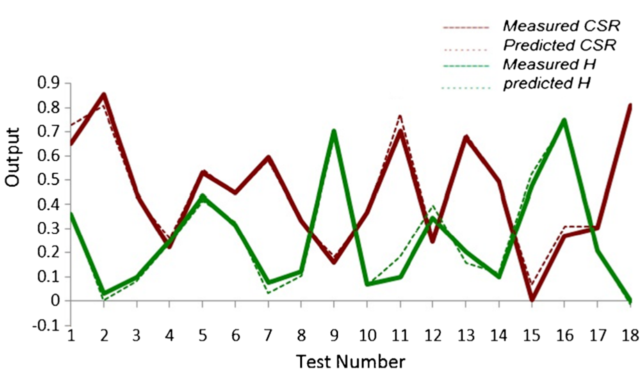

Fig. 6 Comparison between measured and predicted CSR and ΔH for testing datasets for 4–6–2 architecture

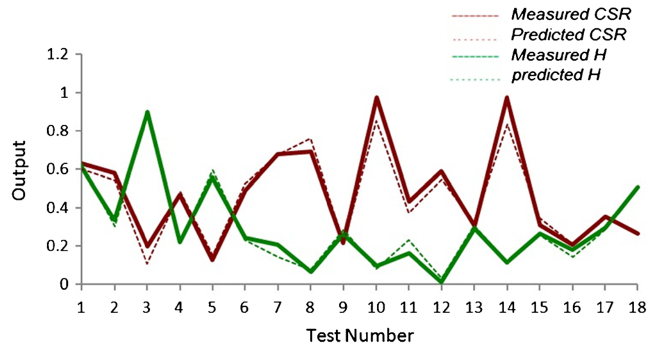

Fig. 7 Comparison between measured and predicted CSR and ΔH for testing datasets for 4–9–2 architecture

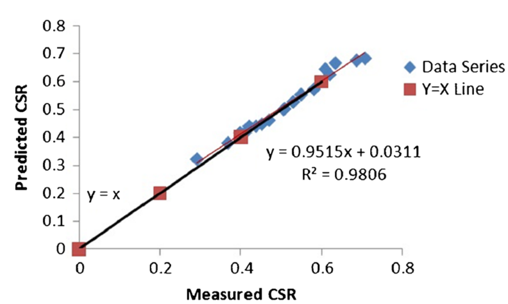

Fig. 8 Correlation between measured and predicted CSR for optimum model (4–6–2)

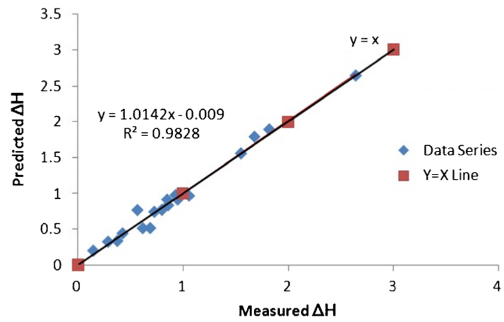

Fig. 9 Correlation between measured and predicted ΔH for optimum model (4–9–2)

Model performance

By comparing predicted and measured values of the collapse settlement and the coefficient of stress release, the performance of constructed models can be easily evaluated. Figures 6 and 7 show the normalized measured and predicted values of both the collapse settlement and the stress release coefficient for 4–6–2 and 4–9–2 model architecture in a single diagram, respectively.

Also, achieving a considerable high value for the coefficient of determination for both models shows the good performance of models. As it can be seen in Figs. 8 and 9, for CSR and ΔH models, R^2 is equal to 0.9806 and 0.9828, respectively. To show the reasonable correlation between measured and predicted values of CSR and ΔH, the line $y=x$ is depicted in addition to the datasets. Also, for CSR optimum model, MAE is equal to 0.013 and for ΔH optimum model, MAE is equal to 0.062.

Sensitivity analysis

In order to attain the most affective factors on the CSR and ΔH, the cosine amplitude method (CAM), is considered (Yang and Zhang 1997; Monjezi et al. 2009). The expressed similarity

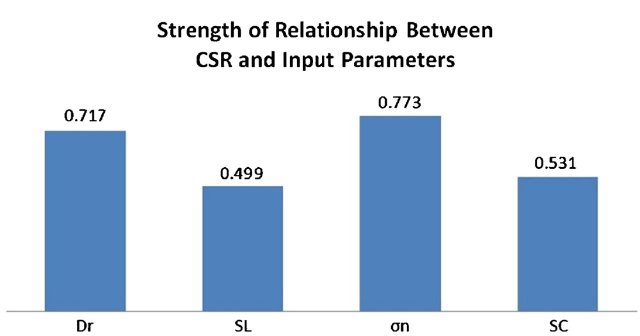

Fig. 10 Sensitivity analysis carried out between CSR and input parameters

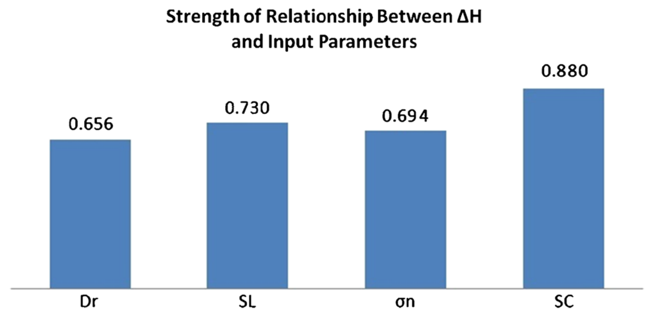

Fig. 11 Sensitivity analysis carried out between ΔH and input parameters

relation between the target function and the input parameters is used to obtain by this method. In this method, all of data pairs are expressed in the common X-space. They would form a data array X defined as Eq. (8) (Yong-Hun and Chung-In 2004; Khandelwal and Singh 2006; Monjezi et al. 2010):

$$X = \{x_1, x_2, x_3, x_4, \ldots, x_i, \ldots x_n\} \tag{8}$$

where each element, x_i, is a vector of the length of m and is shown in Eq. (9).

$$x_i = \{x_{i1}, x_{i2}, x_{3i}, \ldots x_{im}\}. \tag{9}$$

Thus, each of the datasets can be considered as a point in the m-dimensional space, where each point requires m-coordinates to be fully described (Monjezi et al. 2010). The strength of the relationship between x_i and x_j is given by Eq. (10).

$$r_{ij} = \frac{\sum_{k=1}^{m} x_{ik} x_{jk}}{\sqrt{\sum_{k=1}^{m} x_{ik}^2 \sum_{k=1}^{m} x_{jk}^2}}. \tag{10}$$

Regarding this mentioned formula, the strength of the relationship between CSR and input parameters also ΔH and input parameters is shown in Figs. 10 and 11, respectively.

The results show that sand content is the most influential factor on the collapse settlement value, ΔH. Also, the normal stress is the most sensitive parameter affecting on the CSR.

Table 3 The mean and standard deviation of input parameters

Parameter	X	δ
SC	0.5	0.408
σ_n	0.5	0.354
SL	0.482	0.376
Dr	0.467	0.411

Table 4 Parameters used to gain the variation of predicted outputs with inputs

Input				Predicted output	
$X_1-\delta$	X_2	X_3	X_4	$\mathrm{CSR}_{X_1-\delta}$	$\Delta H_{X_1-\delta}$
$X_1-\delta/2$	X_2	X_3	X_4	$\mathrm{CSR}_{X_1-\delta/2}$	$\Delta H_{X_1-\delta/2}$
X_1	X_2	X_3	X_4	CSR_{X_1}	ΔH_{X_1}
$X_1+\delta/2$	X_2	X_3	X_4	$\mathrm{CSR}_{X_1+\delta/2}$	$\Delta H_{X_1+\delta/2}$
$X_1+\delta$	X_2	X_3	X_4	$\mathrm{CSR}_{X_1+\delta}$	$\Delta H_{X_1+\delta}$

Geotechnical interpretation of the network prediction

To well peruse the collapse settlement phenomenon and to ensure the accuracy of trends of predicted outputs, variation of predictions with inputs was studied. In order to study input-predicted output behavior, the mean and standard deviation of each input parameter were calculated using the following equations:

$$X = \frac{\sum x_i}{N} \tag{11}$$

$$\delta = \sqrt{\frac{\sum (x_i - X)^2}{N}} \tag{12}$$

where x_i and N are input parameters and number of datasets, respectively. Also, in these formulas, X and δ, represent the mean and standard deviation of each input parameter for the studied range. Mean and standard deviation of each normalized input parameter are presented in Table 3. To gain the trend of the predicted collapse settlement and the coefficient of stress release with each of inputs, the values of $X-\delta$, $X-\delta/2$, X, $X+\delta/2$, and $X+\delta$ are calculated for each input. Then, the desired outputs are predicted using their optimum models. Table 4 illustrates the mentioned procedure for assessing input-predicted output behavior. In this table, variation of the input X_1 on the collapse parameters is investigated.

Where, the index "i; i=1, … 4" present the mean of i-th input data. For both optimum models, this table is built for all four inputs, separately. Finally, the behavior of the predicted coefficient of stress release and the collapse settlement with change in the value of sand content, normal stress, shear stress level, and relative density is, separately, depicted in Figs. 12 and 13, respectively.

As it can be seen in Figs. 12 and 13, results obtained from the network are efficiently in a good agreement with their real status. In Fig. 12, on one hand, the coefficient of stress release is increased with the increase in the amount of the normal stress and the relative density. On the other hand, it decreases with the increase in the amount of the sand content and the shear stress level.

Also, from Fig. 13, it is clear that the collapse settlement has a direct relationship with the sand content, normal stress, and shear stress level. And, it has an inverse relationship with the relative density.

As a matter of fact, the normal stress with imposing more breakage, the sand content with increasing the inter-grain

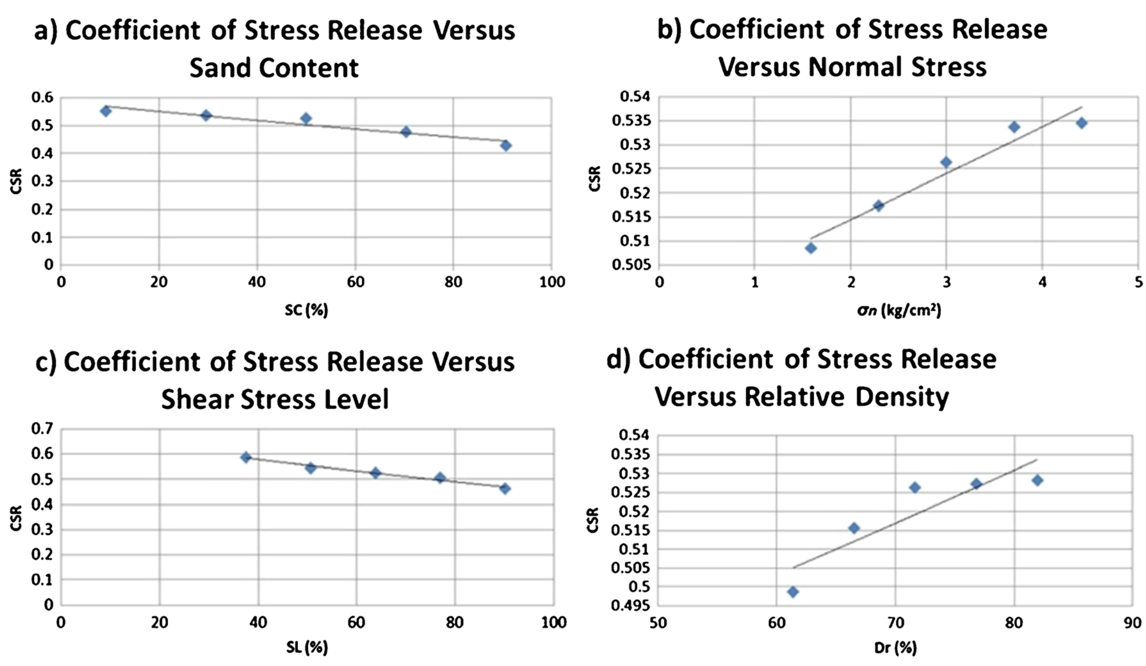

Fig. 12 Variation of coefficient of stress release with input parameters

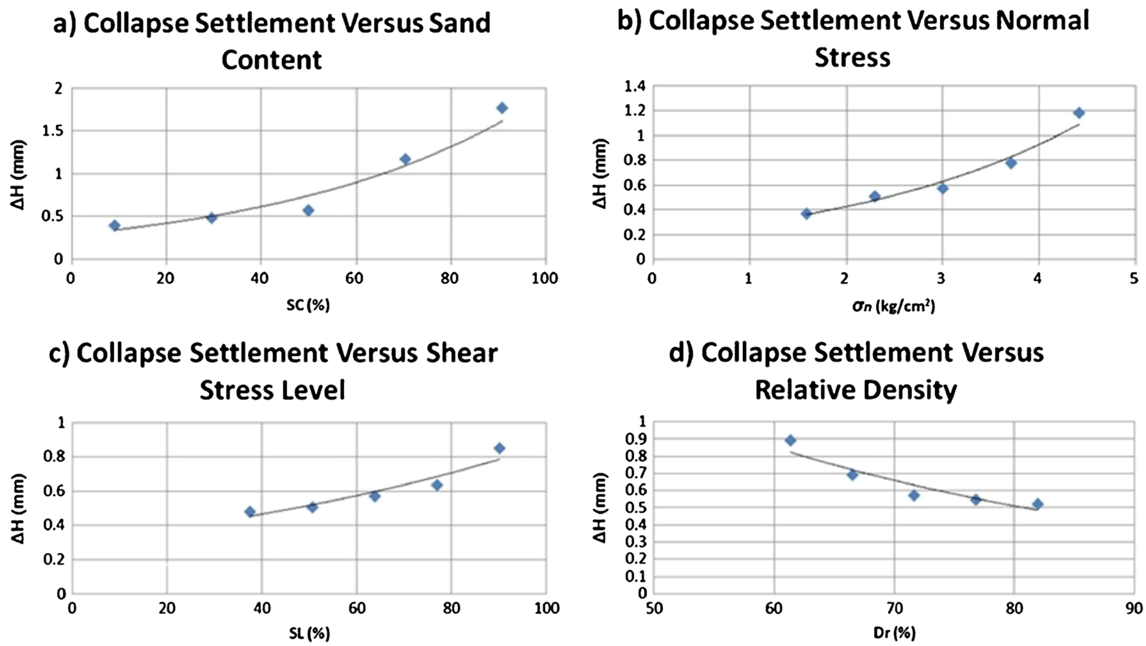

Fig. 13 Variation of ΔH with input parameters

displacement, and stresses and the relative density with increasing the weight of compacted soil in the shear box cause these behaviors, which are plotted in Figs. 12 and 13.

The dependency of the collapse phenomenon to the confining pressure has been observed experimentally and numerically by some researchers (Naderian and Williams 1997; Alizade 2009; Oshtaghi and Mahinroosta 2010; Poorjafar and Mahinroosta 2011). In fact, with increasing the normal stress, the larger amount of collapse settlement occurs, which its trend agrees with the results inferred from Figs. 12b and 13b.

Increasing the relative density in the media results in the better and stiffer contact between soil particles, which leads to fall in the collapse settlement and rise in the stress release coefficient. Also, higher shear stresses induce more micro and possibly macro cracks in rock particles. This facilitates the penetration of water into the cracks, resulting in the breakage and more degradation of the strength and the deformation modulus (Soroush and Aghaeiaraei 2005).

Conclusion

In this study, a new ANN was developed to predict the collapse settlement value and the coefficient of stress release in gravel materials using 180 datasets which were obtained by means of the large-scale direct shear test. Neglecting the parameters with the low variation and those which were constant in this study, four variables were considered as input parameters. Using the sand content, SC, the normal stress, σ_n, the shear stress level, SL, and the relative density, Dr, as input parameters, a feedforward backpropagation method was used to train the datasets. After some trials and based on the comparing the values of RMSE, for different built models, a network with the architecture of 4–6–2 was found as the optimum network in predicting the value of the coefficient of stress release. For this mentioned network, RMSE and the coefficient of determination, R^2, were equal to 0.0171 and 0.981, respectively. Also, an MLP network with the topology 4–9–2 was realized to be the optimum network in predicting the value of the collapse settlement. For this network, the value of the root mean square error and the coefficient of determination were equal to 0.082 and 0.983, respectively. Furthermore, by finding the strength of the relationships between input and output parameters, based on the CAM method, the SC was introduced as the most important parameter and the Dr was the least affective parameter on the collapse settlement value, ΔH. Also, it was observed that the σ_n is the most effective parameter on the coefficient of stress release, whereas the SL was found as the parameter with the least effect on the CSR. Finally, the geotechnical interpretation of the designed network was taken into account. It was shown that all trends in input–output connections are in a good agreement with the basic laws of soil mechanics. Thus, it is shown that besides the well prediction of collapse parameters, the developed ANN is well behaved with the geotechnical engineering considerations.

Appendix 1

Table 5 Data gained by large-scale direct shear test and used in ANN

Input				Output	
SC (%)	σ_n (kg/cm^2)	SL (%)	Dr (%)	CSR	ΔH (mm)
0	1	30	60	0.667	0.12
0	1	50	60	0.578	0.15
0	1	75	60	0.48	0.3
0	1	100	60	0.43	0.61
0	2	30	60	0.685	0.2
0	2	50	60	0.581	0.32
0	2	75	60	0.501	0.4
0	2	100	60	0.431	1.23
0	3	30	60	0.695	0.32
0	3	50	60	0.583	0.42
0	3	75	60	0.502	0.5
0	3	100	60	0.433	1.27
0	4	30	60	0.719	0.45
0	4	50	60	0.589	0.65
0	4	75	60	0.512	0.75
0	4	100	60	0.441	1.3
0	5	30	60	0.723	0.5
0	5	50	60	0.59	0.85
0	5	75	60	0.512	0.91
0	5	100	60	0.444	1.35
50	1	30	60	0.602	0.2
50	1	50	60	0.514	0.3
50	1	75	60	0.452	0.45
50	1	100	60	0.39	0.7
50	2	30	60	0.608	0.3
50	2	50	60	0.516	0.45
50	2	75	60	0.457	0.92
50	2	100	60	0.39	1.1
50	3	30	60	0.608	0.77
50	3	50	60	0.52	0.83
50	3	75	60	0.463	0.95
50	3	100	60	0.39	1.35
50	4	30	60	0.609	0.75
50	4	50	60	0.54	0.91
50	4	75	60	0.483	1.27
50	4	100	60	0.396	1.52
50	5	30	60	0.609	1.12
50	5	50	60	0.541	1.38
50	5	75	60	0.485	1.45
50	5	100	60	0.398	2.28
100	1	30	60	0.558	1.1
100	1	50	60	0.417	1.09
100	1	75	60	0.302	1.25
100	1	100	60	0.289	1.52
100	2	30	60	0.562	1.48

Table 5 (continued)

Input				Output	
SC (%)	σ_n (kg/cm^2)	SL (%)	Dr (%)	CSR	ΔH (mm)
100	2	50	60	0.417	1.6
100	2	75	60	0.346	1.78
100	2	100	60	0.292	2.3
100	3	30	60	0.565	1.89
100	3	50	60	0.419	1.99
100	3	75	60	0.348	2.18
100	3	100	60	0.295	2.64
100	4	30	60	0.587	1.92
100	4	50	60	0.42	2.22
100	4	75	60	0.397	2.34
100	4	100	60	0.376	2.68
100	5	30	60	0.588	1.92
100	5	50	60	0.43	2.35
100	5	75	60	0.398	2.38
100	5	100	60	0.378	2.92
0	1	30	70	0.68	0.12
0	1	50	70	0.58	0.13
0	1	75	70	0.5	0.28
0	1	100	70	0.433	0.55
0	2	30	70	0.708	0.2
0	2	50	70	0.585	0.26
0	2	75	70	0.506	0.39
0	2	100	70	0.437	0.96
0	3	30	70	0.728	0.28
0	3	50	70	0.586	0.36
0	3	75	70	0.508	0.44
0	3	100	70	0.438	0.93
0	4	30	70	0.758	0.4
0	4	50	70	0.61	0.55
0	4	75	70	0.52	0.73
0	4	100	70	0.448	1.05
0	5	30	70	0.769	0.43
0	5	50	70	0.619	0.72
0	5	75	70	0.526	0.82
0	5	100	70	0.45	1.33
50	1	30	70	0.608	0.18
50	1	50	70	0.519	0.27
50	1	75	70	0.465	0.33
50	1	100	70	0.392	0.63
50	2	30	70	0.616	0.29
50	2	50	70	0.53	0.39
50	2	75	70	0.489	0.52
50	2	100	70	0.396	0.85
50	3	30	70	0.628	0.47
50	3	50	70	0.54	0.52
50	3	75	70	0.5	0.65
50	3	100	70	0.41	1.08

Table 5 (continued)

Input				Output	
SC (%)	σ_n (kg/cm^2)	SL (%)	Dr (%)	CSR	ΔH (mm)
50	4	30	70	0.631	0.71
50	4	50	70	0.547	0.87
50	4	75	70	0.509	1.1
50	4	100	70	0.42	1.47
50	5	30	70	0.638	1.07
50	5	50	70	0.549	1.33
50	5	75	70	0.51	1.42
50	5	100	70	0.437	2.1
100	1	30	70	0.566	1.06
100	1	50	70	0.42	1.08
100	1	75	70	0.338	1.23
100	1	100	70	0.289	1.48
100	2	30	70	0.575	1.44
100	2	50	70	0.42	1.55
100	2	75	70	0.351	1.68
100	2	100	70	0.297	2.15
100	3	30	70	0.58	1.84
100	3	50	70	0.424	1.98
100	3	75	70	0.36	2.13
100	3	100	70	0.3	2.59
100	4	30	70	0.592	1.87
100	4	50	70	0.429	2.18
100	4	75	70	0.398	2.25
100	4	100	70	0.386	2.64
100	5	30	70	0.598	1.88
100	5	50	70	0.43	2.3
100	5	75	70	0.4	2.37
100	5	100	70	0.387	2.85
0	1	30	85	0.687	0.11
0	1	50	85	0.581	0.12
0	1	75	85	0.505	0.28
0	1	100	85	0.435	0.5
0	2	30	85	0.712	0.2
0	2	50	85	0.585	0.2
0	2	75	85	0.508	0.38
0	2	100	85	0.437	0.7
0	3	30	85	0.731	0.28
0	3	50	85	0.59	0.34
0	3	75	85	0.511	0.42
0	3	100	85	0.44	0.86
0	4	30	85	0.768	0.38
0	4	50	85	0.619	0.5
0	4	75	85	0.527	0.71
0	4	100	85	0.452	0.98
0	5	30	85	0.779	0.42
0	5	50	85	0.621	0.69
0	5	75	85	0.53	0.8

Table 5 (continued)

Input				Output	
SC (%)	σ_n (kg/cm^2)	SL (%)	Dr (%)	CSR	ΔH (mm)
0	5	100	85	0.453	1.33
50	1	30	85	0.615	0.18
50	1	50	85	0.522	0.27
50	1	75	85	0.47	0.3
50	1	100	85	0.392	0.62
50	2	30	85	0.629	0.29
50	2	50	85	0.538	0.36
50	2	75	85	0.5	0.44
50	2	100	85	0.398	0.8
50	3	30	85	0.635	0.39
50	3	50	85	0.544	0.45
50	3	75	85	0.502	0.57
50	3	100	85	0.41	0.97
50	4	30	85	0.64	0.7
50	4	50	85	0.549	0.87
50	4	75	85	0.509	0.99
50	4	100	85	0.428	1.45
50	5	30	85	0.642	1.02
50	5	50	85	0.553	1.29
50	5	75	85	0.511	1.4
50	5	100	85	0.44	1.93
100	1	30	85	0.573	1.06
100	1	50	85	0.422	1.07
100	1	75	85	0.351	1.23
100	1	100	85	0.291	1.45
100	2	30	85	0.585	1.43
100	2	50	85	0.425	1.52
100	2	75	85	0.362	1.66
100	2	100	85	0.3	2
100	3	30	85	0.591	1.8
100	3	50	85	0.427	1.98
100	3	75	85	0.368	2.09
100	3	100	85	0.302	2.54
100	4	30	85	0.597	1.82
100	4	50	85	0.434	2.15
100	4	75	85	0.398	2.2
100	4	100	85	0.386	2.6
100	5	30	85	0.598	1.85
100	5	50	85	0.435	2.25
100	5	75	85	0.401	2.36
100	5	100	85	0.387	2.8

References

Alizade A (2009) Numerical modeling of collapse settlement in rockfill dams due to saturation. M.Sc. Dissertation, Zanjan University, Zanjan, Iran

Alonso EE (2003) Exploring the limits of unsaturated soil mechanics: the behavior of coarse granular soil and rockfill. The Eleventh Spencer J. Buchanan Lecture. College Station Hilton. 1–53

Alonso EE, Oldecop LA (2000) Fundamentals of rockfill collapse. In: Rahardjo H, Toll DG and Leong EC (eds) Unsaturated soils for Asia. Proceedings of the 1st Asian Conference on Unsaturated Soils (UNSAT-ASIA 2000). Singapore, Balkema, Rotterdam. 3–13

Asadzadeh M, Soroush A (2009) Direct shear testing on a rockfill material. Arab J Sci Eng 34(2B):379–396

Basma AA, Kallas N (2004) Modeling soil collapse by artificial neural networks. J Geotech Geol Eng 22(3):427–438. doi:10.1023/B:GEGE.0000025044.72718.db

Baumann P (1958) Rockfill dams: Cogswell and San Gabriel dams. ASCE J Power Div 84(3):1–33

Demuth H, Beal M, Hagan M (1996) Neural network toolbox 5 user's guide. The Math Work, Inc, Natick

Farmer IW, Attewell PB (1973) The effect of particle strength on the compression of crushed aggregates. Rock Mech 5:237–248, Springer-Verlag

Feda J (1995) Mechanisms of collapse of soil structure. In: Derbyshire E et al (eds) Genesis and properties of collapsible soils. Proc. workshop, Loughborough, 1994. NATO ASI Series C, 468, Kluwer, p 149–172

Funahashi K (1989) On the approximate realization of continuous mappings by neural networks. J Neural Netw 2(3):183–192

Habibagahi G, Taherian M (2001) Prediction of collapse potential via artificial neural networks. Proc. of the 6th Int. Conf. on Application of Artificial Intelligence to Civil and Structural Engineering, Vienna. Paper 33

Haeri SM, Zamani A, Garakani AA (2012) Collapse potential and permeability of undisturbed and remolded loessial soil samples. Unsaturated Soils: Res Appl 1:301–308. doi:10.1007/978-3-642-31116-1_41

Hasanzadehshooiili H, Lakirouhani A, Sapalas A (2012a) Neural network prediction of buckling load of steel arch-shells. Arch Civ Mech Eng 12(4):477–484, http://dx.doi.org/10.1016/j.acme.2012.07.005

Hasanzadehshooiili H, Lakirouhani A, Medzvieckas J (2012b) Superiority of artificial neural networks over statistical methods in prediction of the optimal length of rock bolts. J Civ Eng Manag 18(5):655–661. doi:10.3846/13923730.2012.724029

Hornik K (1989) Multilayer feedforward networks are universal approximators. J Neural Netw 2:359–366

Hornik K (1991) Approximation capabilities of multi layer feed forward networks. Neural Netw J 4:251–257

Hunter G (2002) The deformation behavior of rockfill. Journal of Geotechnical and Environmental Engineering. UNICIV Report, Issue 10, No. R-405

Juang CH, Elton DJ (1997) Predicting collapse potential of soils with neural networks. Transportation research record. J Transp Res Boar Soils Geol Found Category 1582:22–28. doi:10.3141/1582-04

Justo JL (1991) Test fills and in situ tests. In: Maranha das Neves E (ed) Advances in rockfill structures, 153-193. doi:10.1007/978-94-011-3206-0_7

Kakoli STN, Hanna AM (2011) Causes of foundation failure and sudden volume reduction of collapsible soil during inundation. In: Noor, Amin, Bhuiyan, Chowdhury and Kakoli (eds) 4th Annual Paper Meet and 1st Civil Engineering Congress, December 22–24, 2011, Dhaka, Bangladesh. ISBN: 978-984-33-4363-5.

Khandelwal M, Singh TN (2006) Prediction of blast induced ground vibrations and frequency in opencast mine—a neural network approach. J Sound Vib 289:711–725

Khandelwal M, Roy MP, Singh PK (2004) Application of artificial neural network in mining industry. Indian Min Eng J 43(7):19–23

Kim BS, Park SW, Kato S (2012) DEM simulation of collapse behaviours of unsaturated granular materials under general stress states. Comput Geotech 42:52–61, http://dx.doi.org/10.1016/j.compgeo.2011.12.010

Marachi ND, Chan CK, Seed HB, Duncan JM (1969) Strength and deformation characteristics of rockfill materials. Report No. TE-69-5. University of California. Department of Civil Engineering

Marsal RJ (1967) Large scale testing of rockfill material. J Soil Mech Found Div ASCE 93(SM2):27–43

Marsal RL (1973) Mechanical properties of rockfill. In: Hirschfeld RC, Poulos SJ (eds) Embankment dam engineering (Casagrande volume). Wiley, New York, pp 109–200

Maulenkamp F, Grima MA (1999) Application of neural networks for the prediction of the unconfined compressive strength (UCS) from Equotip hardness. Int J Rock Mech Min Sci 36:29–39

McCulloch WS, Pitts W (1988) A logical calculus of the ideas immanent in nervous activity. Bull Math Biophys 5:115–133

Monjezi M, Dehghani H (2008) Evaluation of effect of blasting pattern parameters on backbreak using neural networks. Int J Rock Mech Min Sci 45:1446–1453

Monjezi M, Bahrami A, Yazdian A, Sayadi AR (2009) Prediction and controlling of flyrock in blasting operation using artificial neural network. Arab J Geosci. doi:10.1007/s12517-009-0091-8

Monjezi M, Aminikhoshalan H, Yazdianvarjani A (2010) Prediction of flyrock and backbreak in open pit blasting operation: a neuro-genetic approach. Arab J Geosci. doi:10.1007/s12517-010-0185-3

Naderian AR, Williams DJ (1997) Bearing capacity of open coal-mine backfill materials. Trans. Instn Min Metall. The Institution of Mining and Metallurgy. A30–A34

Naylor DJ (1997) Collapse settlement—some developments. In: Azevedo et al (eds) Application of computational mechanics in geotechnical engineering. Balkema, Rotterdam

Neaupane KM, Adhikari NR (2006) Prediction of tunneling-induced ground movement with the multi-layer perceptron. Int J Tunn Undergr Space Technol 21:15–159

Oshtaghi V, Mahinroosta R (2010) Changes in the stress and strain state in dry gravelly material due to saturation. 4th International Conference on Geotechnical Engineering and Soil Mechanics. Tehran. Iran. Paper No. TVTMAH 190

Pearson DW, Steele NC, Albrecht RF (1995) Artificial neural nets and genetic algorithms. In: Proceedings of the International Conference in Ales, France, 333–336

Poorjafar A, Mahinroosta R (2011) Investigation of collapse settlement in sandy soils with triaxial shear test. 6th Iranian National Congress on Civil Engineering. Semnan, Iran

Rosenblatt F (1988) The perceptron: a probabilistic model for information storage and organization in the brain. Psychol Rev 65:386–408

Simpson PK (1990) Artificial neural system: foundation, paradigms, applications and implementations. Pergamon, New York, p 18

Soriano A, Sánchez FJ (1999) Settlements of railroad high embankments. Proc. XII European Conf. On Soil Mech. and Geotech. Eng. Netherlands

Soroush A, Aghaeiaraei A (2005) Uncertainties in mechanical behavior of rockfill during first impounding of rockfill dams. 73rd Annual Meeting of Icold. Tehran, Iran

Soroush A, Aghaeiaraei A (2009) Analysis of behavior of a high rockfill dam. Proceeding of the Institution of Civil Engineering. Geotechnical Engineering. 159 (GEI), 49–59

Terzaghi K (1960) Discussion on 1958 paper by Steele & Cooke: Rockfill dams: Salt springs and Lower Bear River concrete face dams. ASCE Trans 125(2):139–148

Touileb BN, Bonelli S, Anthiniac P, Carrere A, Debordes O, Berbera GLA, Bani A, Mazza G (2000) Settlement by wetting of the upstream rockfills of large dams. Proc. of the 53rd Canadian Geotechnical Conf. Montreal. 263–270

Yang Y, Rosenbaum MS (2002) The artificial neural network as a tool for assessing geotechnical properties. Geotech Geol Eng 20:149–168

Yang Y, Zhang Q (1997) Analysis for the results of point load testing with artificial neural network. In: Proceedings of the computer methods and advances in geomechanics. IACMAG. China. 607–612

Yasrebi SSH, Emami M (2008) Application of artificial neural networks (ANNs) in prediction and interpretation of pressure meter test results. The 12th International Conference of International Association for Computer Methods and Advances in Geomechanics (IACMAG). 1–6 October. Goa, India

Yong-Hun J, Chung-In L (2004) Influence of geological conditions on the powder factor for tunnel blasting. Int J Rock Mech Min Sci 41:533–538

Yuan-Ping J, Xiao-Yan H (2007) Feasibility study on soil collapse simulation with artificial neural network model. Journal of Yangtze University (Natural Science Edition) Sci & Eng V. 2007–02. http://en.cnki.com.cn/Article_en/CJFDTOTAL-CJDL200702034.htm